Three Archetypical Classes of Macromolecular Regulators of Protein Liquid-Liquid Phase Separation

Short title: Three classes of LLPS regulators

Archishman Ghosh[a,b], Konstantinos Mazarakos[b], and Huan-Xiang Zhou[b,*]

[a]Institute of Molecular Biophysics, Florida State University, Tallahassee, FL 32306, USA

[b]Department of Chemistry and Department of Physics, University of Illinois at Chicago, Chicago, IL 60607, USA

*To whom correspondence should be addressed. E-mail: hzhou43@uic.edu.

Supporting Information

www.pnas.org/cgi/doi/10.1073/pnas.1907849116

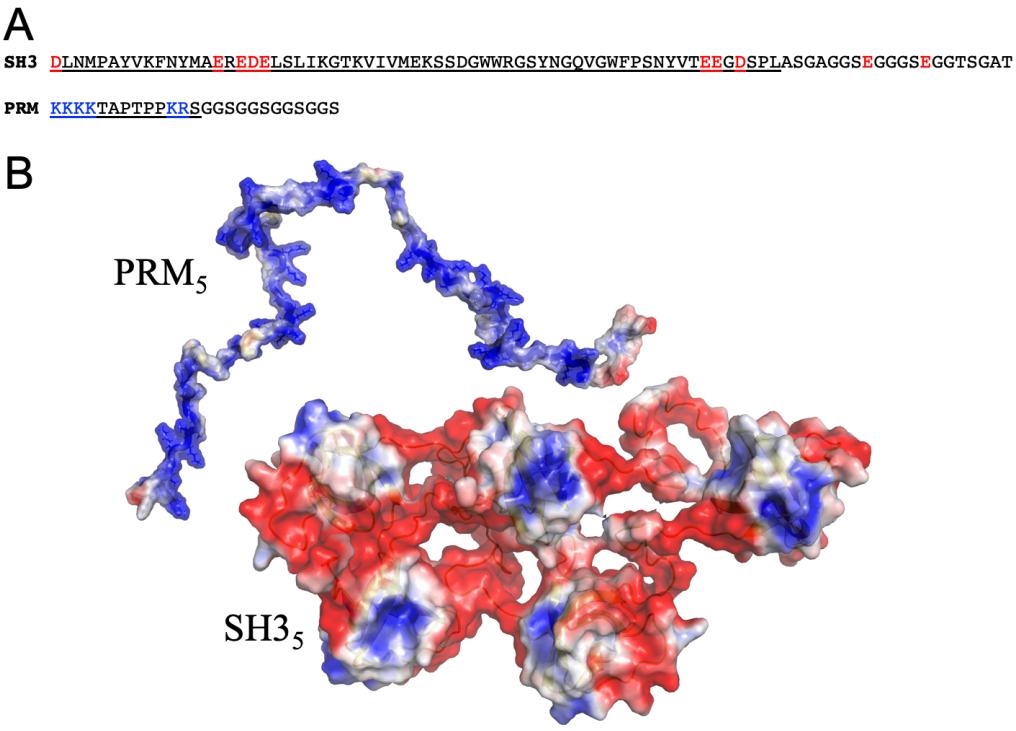

Fig. S1. Sequences and electrostatic surfaces of $SH3_5$ and PRM_5. (*A*) Sequence of a single module of $SH3_5$ or PRM_5. For the SH3 module, the sequence of the SH3 domain is underlined and that of the inter-SH3 linker is not. Anionic residues contributing to a strong negative electrostatic surface are indicated in red. In the full $SH3_5$ construct, the first module was preceded by three residues (GHM) and the third module by two residues (HM); the fifth module had the inter-SH3 linker replaced by the sequence ENLYFQ. For the PRM module, the sequence of the proline-rich motif recognized by SH3 domains is underlined and that of the inter-PRM linker is not. Cationic residues contributing to a strong positive electrostatic surface are indicated in blue. In the full PRM_5 construct, the first module was preceded by the sequence GHMKGGSWGGS, and the fifth module had the inter-PRM linker replaced by the sequence GGSGSENLYFQ. (*B*) Electrostatic surfaces of $SH3_5$ or PRM_5. Blue and red colors indicate positive and negative electrostatic potentials, respectively.

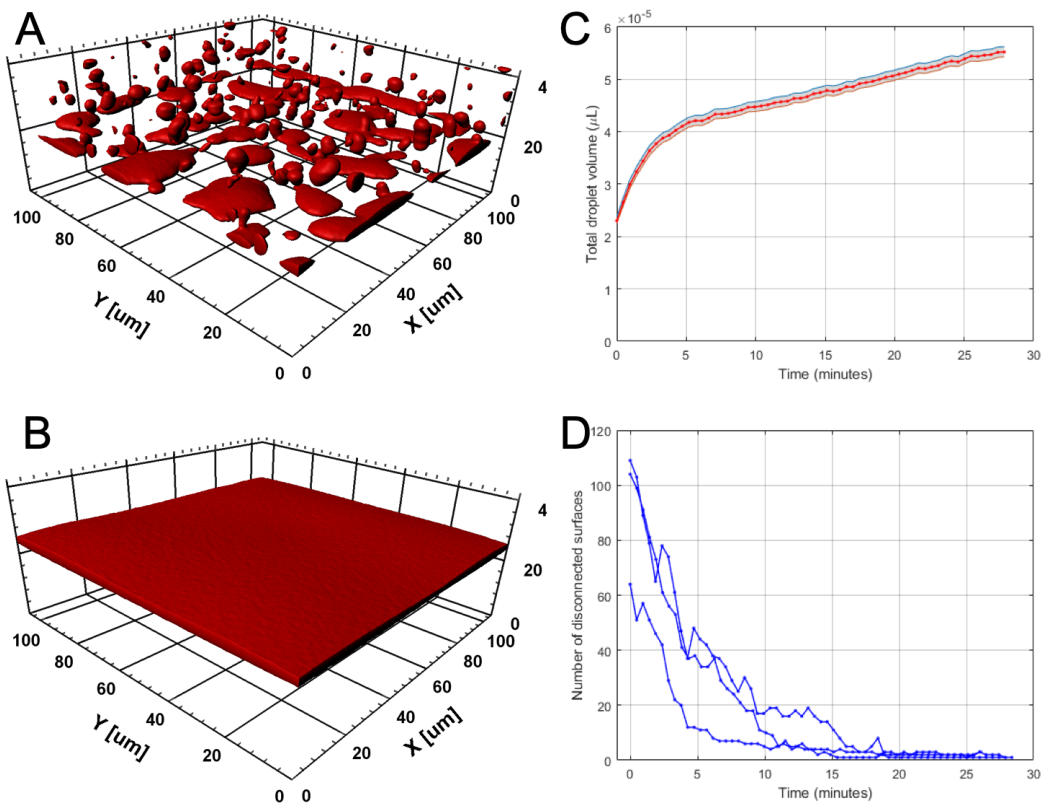

Fig. S2. Falling, coalescence, and spread of $SH3_5$-PRM_5 droplets over a coverslip. (*A*, *B*) Rendered surfaces of the droplet phase in the first and last Z-stacks (former shown in Fig. 2*B*) in a time series collected over 28 min, after a 1.5 µl sample containing 40 µM each of $SH3_5$ and PRM_5 and 1 µM Alexa594-$SH3_5$ was mounted on the microscope. Each of the 60 Z-stacks covered an area of 105 µm × 105 µm and a depth of 40 µm. (*C*) The total volume of the droplet phase in each Z-stack. The shaded band indicates uncertainty in choosing an intensity threshold for best match between the surface rendering and the original image. This uncertainty is much less than the variation in droplet volume between repeat experiments. Note that nearly half of the total droplet volume was accumulated within 40 µm of the coverslip by the time the first Z-stack was scanned, indicating that significant falling of droplets already took place within the less than 20-second "deadtime". (*D*) The number of disconnected surfaces in each of the 60 Z-stacks, shown for three repeat experiments.

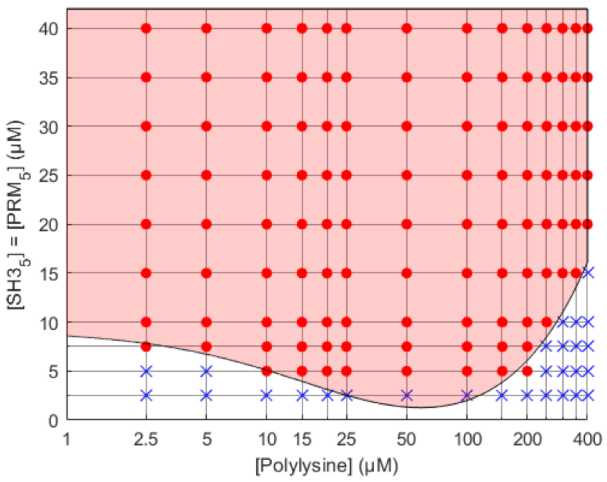

Fig. S3. Regulatory effect of polylysine on the phase boundary of equimolar $SH3_5$-PRM_5 mixtures. The curve separating the phase-separated and non–phase-separated regions is given by the following equation: $y = (0.054x^2 - 5.08x + 216.2)/(x + 23.6)$.

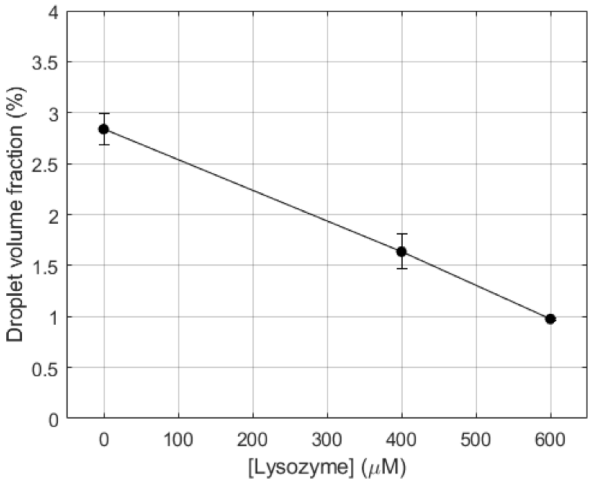

Fig. S4. Effect of lysozyme on the droplet volume fraction. A decrease in droplet volume fraction indicates suppression of phase separation.

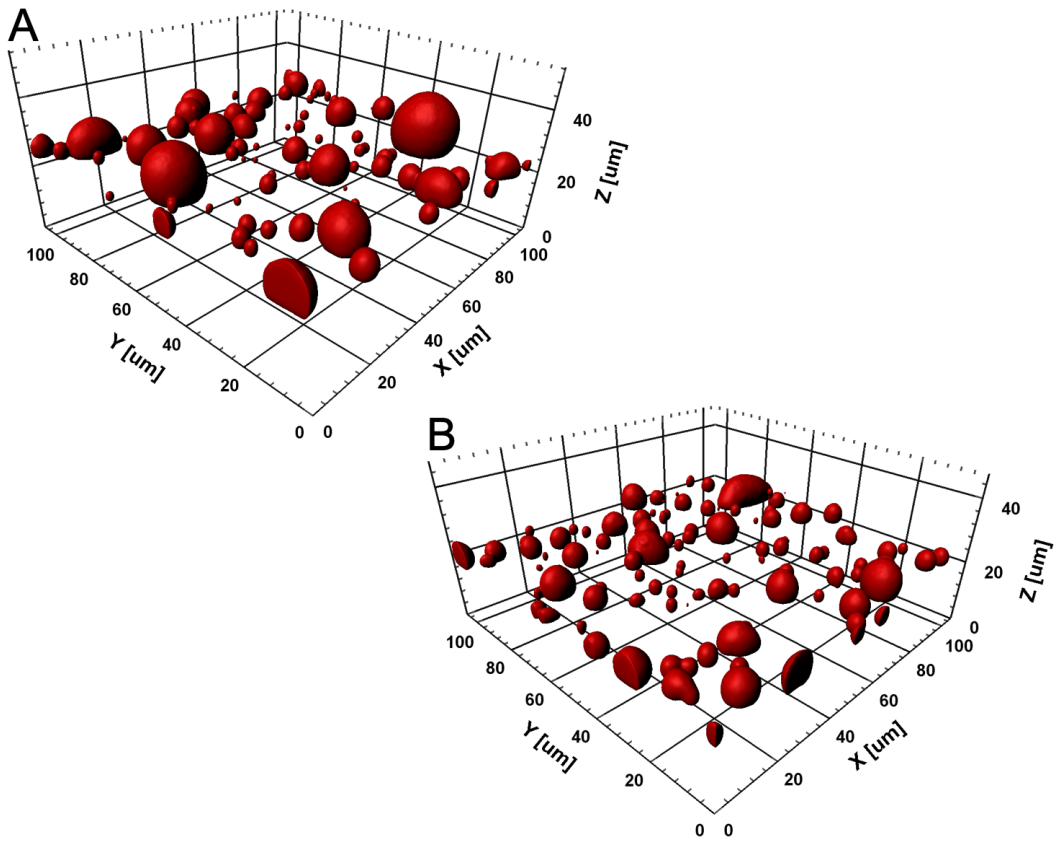

Fig. S5. Rendered surfaces of the droplet phase in the last Z-stacks in a time series collected over 28 min, scanned inside a 1.5 µl sample containing 40 µM each of $SH3_5$ and PRM_5, 1 µM Alexa594-$SH3_5$, and (*A*) 400 µM and (*B*) 600 µM lysozyme. Note the decrease in droplet volume fraction with increasing lysozyme concentration. Also, compared to the counterpart in the absence of lysozyme (Fig. S2*A*), the droplet phase in the presence of lysozyme did not spread over the coverslip, indicating an increase in surface tension.

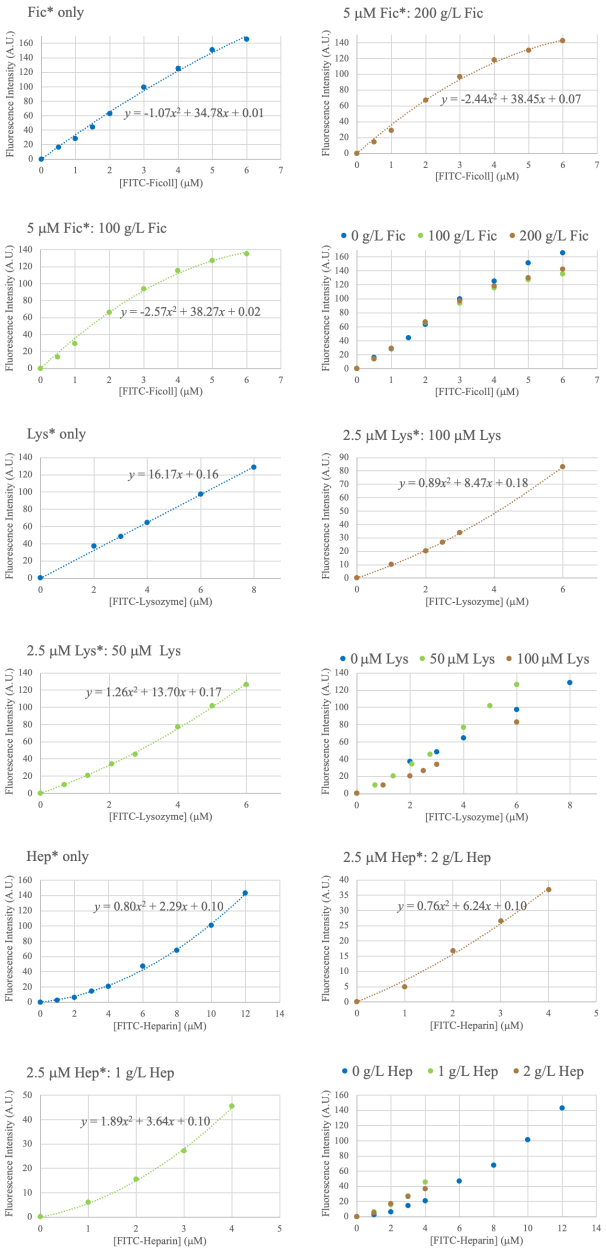

Fig. S6. Standard curves for regulators. Data points in each curve maintained a constant ratio between the labelled (marked with a *) and unlabeled species, and were fitted to either a linear or a quadratic dependence on the labeled regulator concentration. (Abbreviations: Fic = Ficoll70, Lys = lysozyme, Hep = heparin.) For each regulator, standard curves were determined at three labeled to unlabeled ratios, and the three sets of data points are overlaid in a fourth panel to demonstrate that the amount of unlabeled species can affect the standard curve.

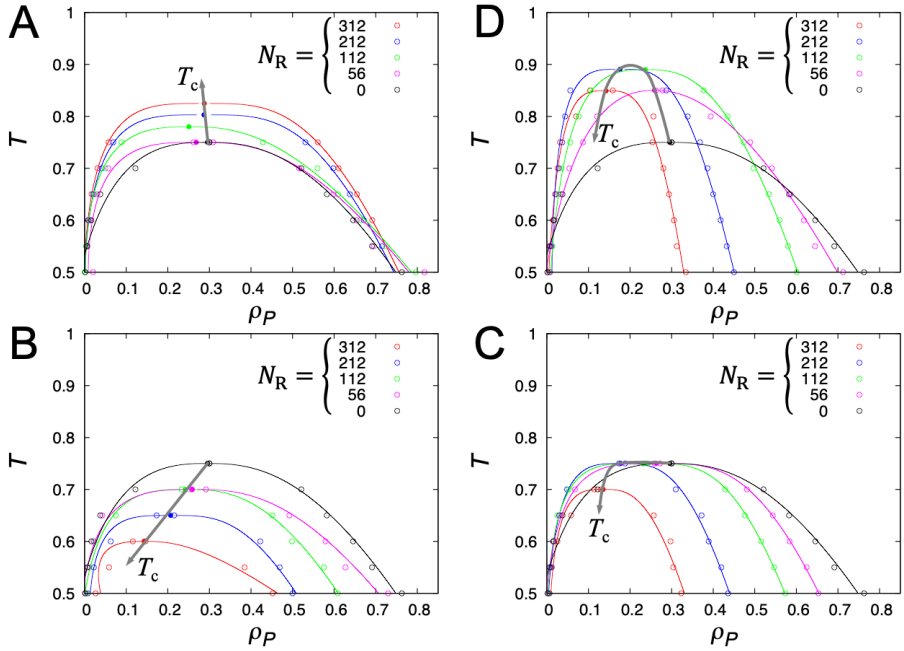

Fig. S7. Phase diagrams of patchy particle models of ternary mixtures at 1:1 driver-driver molar ratio. The strengths (ε_{1R}) of driver 1-regulator attraction were: (*A*) 0; (*B*) 1.0; (*C*) 1.5; and (*D*) 2.0. The trends of T_c (arrowed curves) at increasing particle number (N_R) of the regulator indicate the regulatory effects as volume-exclusion promotion at $\varepsilon_{1R} = 0$, weak-attraction suppression at $\varepsilon_{1R} = 1.0$, and strong-attraction promotion at $\varepsilon_{1R} = 2.0$. At $\varepsilon_{1R} = 1.5$, T_c were flat until $N_R = 212$ (corresponding to a molar fraction of 0.41), suggesting that this ε_{1R} value is close to the upper bound for weak-attraction suppression.

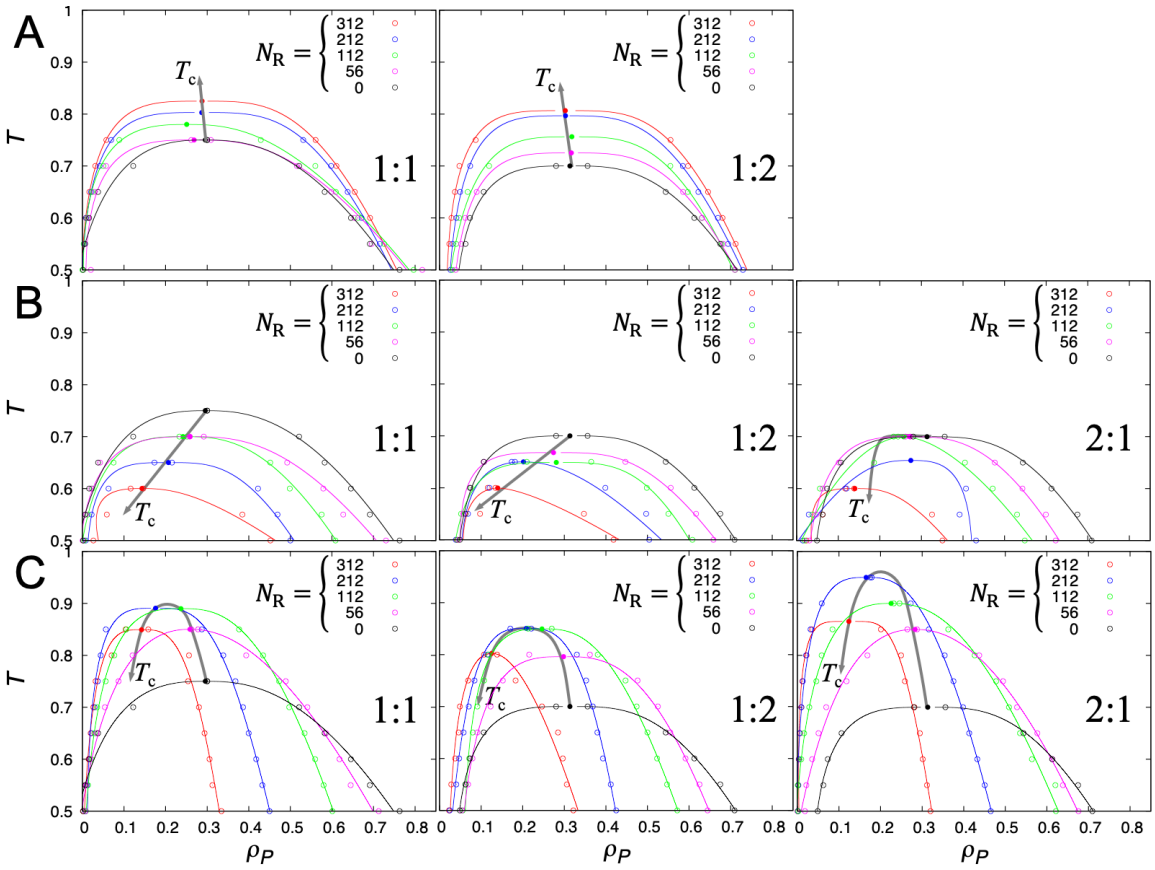

Fig. S8. Phase diagrams of patchy particle models of ternary mixtures at 1:1, 1:2, and 2:1 driver-driver molar ratio. The strengths (ε_{1R}) of driver 1-regulator attraction were: (*A*) 0; (*B*) 1.0; and (*D*) 2.0. The results at ε_{1R} = 1.5 are presented in Fig. 7*A*. Note that at ε_{1R} = 0, there is no difference between 1:2 and 2:1 mixtures, and so only the 1:2 results are shown.